

Thermal Stability of Ag Films with Various Interface Layers

Ziyang Zhang, Midori Kawamura*, Yoshio Abe, and Kyung Ho Kim

Department of Materials Science and Engineering, Kitami Institute of Technology, 165
Koen-cho, Kitami, Hokkaido 090-8507, Japan

Abstract

The effects of Pd, Ni, Nb, and Ti interface layers on the thermal stability of Ag films were investigated, and those metals that are appropriate for the interface layers were summarized. The results indicated that Ti and Nb interface layers resulted in thermally stable Ag films by improving the adhesion strength of the Ag films to SiO₂ substrates and by enhancing the crystal orientation of Ag(111). It was determined that appropriate interface layer metals for Ag film should have a large Gibbs free energy of formation for the oxide and an appropriate atomic diameter ratio of $d_{\text{metal}}/d_{\text{Ag}}$.

Keywords: Ag film, Interface layer, Thermal stability, Adhesion, Crystal orientation

Silver (Ag) is useful as reflective coating or electrode in various electronic devices due to its high optical reflectance or low electrical resistivity.^{1, 2)} However, severe agglomeration of Ag films easily occurs by heating, which causes a significant increase in the electrical resistivity and a drop of the reflectance. It has been reported that the ease of surface Ag diffusion and the poor adhesion of Ag films to oxide substrates are considered to be inherent reasons for the agglomeration.³⁻⁵⁾ Recently, we have summarized appropriate metal surface layer for the suppression of Ag agglomeration.⁶⁾ Namely, it has been found that high cohesive energy or high Gibbs free energy of formation of the oxide ($\Delta_f G^{\circ}_{\text{oxide}}$) and a low solid solubility in Ag are important. Similarly, the insertion of a metallic interface layer has been considered to be a reasonable solution to the agglomeration issue as well as a metal oxide layer.⁷⁾ The use of the metallic interface layer could improve the adhesion strength between the Ag film and the substrate, and/or enhance the crystal orientation of Ag(111) to decrease the surface energy. However, there has been little further work reported that details the types of metals that are appropriate for use as the interface layers for Ag films. In the present work, palladium (Pd), nickel (Ni), niobium (Nb), and titanium (Ti) were selected as interface layer metals for investigation, because they have different properties, such as $\Delta_f G^{\circ}_{\text{oxide}}$ ⁸⁾, crystal structure and nearest-neighbor distance⁹⁾, as shown in Table 1, which are considered to be closely related to the desired roles of these interface layers.

Single-layer Ag (100 nm) film and Ag (100 nm) films with various interface layers (5 nm thick) of Pd, Ni, Nb, and Ti were deposited using rf magnetron sputtering in an Ar atmosphere. The purities of the Ag, Pd, Ni, Nb, and Ti targets were all 99.99%. A Si (001) wafer with a 100 nm thick thermally grown SiO₂ layer was used as a substrate

without heating during deposition. Sputtering of Ag, Pd, Nb, or Ti was conducted with the gas pressure fixed at 1.3 Pa, the target-substrate distance fixed at 55 mm, and the rf power at 15–30 W. However, for sputtering of the Ni interface layer, the gas pressure and rf power were increased to 3.7 Pa and 100 W, respectively, and the target-substrate distance was shortened to 40 mm, because magnetic Ni does not form a plasma as easily as non-magnetic metals by magnetron sputtering.¹⁰⁾ Annealing treatment was performed at 600 °C in a lamp-heating furnace for 1 h after evacuation to less than 1.0×10^{-4} Pa. Scanning electron microscopy (SEM) and atomic force microscopy (AFM) were employed to observe the surface morphology of the films, and the rms surface roughness was calculated through AFM analysis. Micro-scratch testing (scratch speed: 10 $\mu\text{m/s}$; loading rate: 2.67 mN/s) was conducted to evaluate the adhesion of the film on the SiO_2 substrate. The crystal structure was determined by X-ray diffraction (XRD) analysis using $\text{Cu K}\alpha$ radiation.

Figure 1 shows SEM images of the single-layer Ag film and Ag films with various interface layers after annealing at 600 °C. All of the as-deposited films had very smooth surfaces (data not shown here). After the annealing, the single-layer Ag film was agglomerated and the substrate was partly exposed, as shown in Fig. 1(a). However, the inserting of various interface layers improved the morphological stability of the Ag films to varying degrees. Very large voids with diameters of about 5 μm were formed in the Ag/Pd film, as shown in Fig. 1(b), and AFM analysis shows that the rms surface roughness was 9.2 nm, except where there were voids. Therefore, the Pd interface layer has little effect in suppressing Ag agglomeration. In the Ag/Ni film (Fig. 1(c)), the size of the voids was less than a quarter of that in the Ag/Pd film, which suggests that the effect of the Ni interface layer to suppress agglomeration is slightly better than that of

the Pd interface layer. However, there were still a large number of voids in the Ag/Ni film. The introduction of Nb or Ti interface layers resulted in much fewer voids and the rms roughness of the Ag/Nb (Fig. 1(d)) and Ag/Ti (Fig. 1(e)) films decreased to 5.4 and 3.4 nm, respectively. This indicates that the morphological stability of the Ag films can be significantly improved by the implementation of Nb and Ti interface layers, especially the Ti interface layer, which is considered to be the optimum layer by comparison.

The main roles of the interface layer are discussed in detail. Figure 2 shows the critical delamination load of the as-deposited films, which was measured by micro-scratch testing to evaluate the adhesion strength of the film to the substrate. As a result, it is found that insertion of Ni, Nb, and Ti interface layers increases the adhesion strength of the Ag films to the SiO₂ substrates to more than four times that of the single-layer Ag film. However, the use of the Pd interface layer has little influence on the adhesion characteristics. As shown in Table 1, Nb and Ti possess very large $\Delta_f G^{\circ}_{\text{oxide}}$, so the layers of these metals easily forms strong bonds with SiO₂ substrate due to the strong affinity of the metal atoms for the oxygen. In addition, the increased adhesion caused by the Ni interface layer may be attributed to the higher rf power and the shorter target-substrate distance used during deposition. Furthermore, strong metallic bonds can be formed at the interface with the Ag film. Therefore, the Ni, Nb, and Ti interface layers with large $\Delta_f G^{\circ}_{\text{oxide}}$ (Table 1) could improve the adhesion of the Ag films to the SiO₂ substrate. In contrast, noble metals such as Ag, Pd exhibit poor adhesion to the SiO₂ substrate, due to their low $\Delta_f G^{\circ}_{\text{oxide}}$. It is considered that the improved adhesion strength between the Ag film and SiO₂ substrate with the use of appropriate interface layers reduces the interfacial energy, which is beneficial to improve the thermal stability

of the Ag film. Peden *et al.* reported that interfacial interaction of thin films of Cr, Fe, Ni, or Cu on an oxide layer which was assessed by temperature programmed desorption experiments follows the heats of formation of the oxides of those metals.¹¹⁾ In the present study, we have revealed the relation by measuring the interaction more directly.

Figure 3 shows XRD patterns of θ - 2θ scan and rocking curves for the as-deposited films. Insertion of Nb or Ti interface layers results in a much stronger Ag(111) peak intensity than that for the single-layer Ag film, and the disappearance of the Ag(200) peak, as shown in Fig. 3(a). This means that the Ag film deposited on Nb or Ti interface layers has a single orientation. However, the Ag/Pd and Ag/Ni films exhibit both Ag(111) and Ag(200) orientations as for the single-layer Ag film, although the Ag(111) peaks are slightly higher and the Ag(200) peaks are slightly lower than those for the single-layer Ag film. The full width at half maximum (FWHM) of the XRD rocking curves (Fig. 3(b)) was also investigated to evaluate the crystal orientation of Ag(111). The Ag/Nb and Ag/Ti films exhibited a very high Ag(111) crystal orientation, with Ag/Ti as the most highly oriented, whereas the Pd and Ni interface layers had no significant influence on the crystal orientation of Ag(111). The surface energies of the Ag(110), (100), and (111) planes are known to be 1.238, 1.200, and 1.172 J/m², respectively.¹²⁾ Therefore, Ag films with a higher (111) crystal orientation, such as the Ag/Nb and Ag/Ti films, have lower surface energy, which contributes to the improvement in the thermal stability of the film. From these results, it is concluded that the Ag/Nb and Ag/Ti films exhibit better thermal stability than the Ag/Ni and Ag/Pd films due to the combined effect of strong adhesion to the SiO₂ substrate and the high crystal orientation of Ag(111), and as such, the Ti interface layer in particular achieves the best result.

The mechanism for the change in the Ag(111) orientation with the various interface layers is discussed. Table 1 shows that Ag, Pd, and Ni have a fcc structure, Nb has a bcc structure, and Ti has a hcp structure. It has been confirmed that single-layer Pd, Ni, Nb, and Ti films deposited on SiO₂ substrates exhibit a preferential orientation of their respective close-packed planes. Note that any three neighboring atoms closely link and form an equilateral triangle in the close-packed planes of fcc(111) and hcp(0001). Thus, considering that the nearest-neighbor distances for Ag and Ti are both 0.289 nm, as shown in Table 1, the Ag(111) plane can be easily located on the Ti(0001) plane. However, the nearest-neighbor distances for Pd (0.275 nm) and Ni (0.249 nm) do not match well with that for Ag; therefore, the crystal orientation of Ag(111) was not improved on these metal layers. The nearest-neighbor distance has been considered to be the diameter of a metal atom, d_{metal} . Thus, an atomic diameter ratio of $d_{\text{metal}}/d_{\text{Ag}} \approx 1$ is important for metals with a fcc or hcp structure to improve the orientation of Ag(111). In addition, it has been reported that it is difficult for fcc(111) planes to arrange on bcc(110) planes unless the Nishiyama-Wassermann (NW)^{13, 14)} or Kurdjumov-Sachs (KS)¹⁵⁾ relationships are satisfactory^{16, 17)}. For the NW case, the optimal ratio is $d_{\text{bcc}}/d_{\text{fcc}} = 0.866$ or 1.061 , whereas that for the KS case is $d_{\text{bcc}}/d_{\text{fcc}} = 0.919$. For an atomic diameter ratio close to one of these values, the corresponding orientation is usually observed.¹⁸⁾ The atomic diameter ratio for $d_{\text{Nb}}/d_{\text{Ag}}$ is determined to be 0.990, which is close to both 1.061 and 0.919, which indicates that it is possible for a Ag film on a Nb interface layer to grow according to the NW or/and KS path. However, the atomic diameter ratio for $d_{\text{Ti}}/d_{\text{Ag}}$ is closer to the ideal value than that for $d_{\text{Nb}}/d_{\text{Ag}}$; therefore, the effect of the Ti interface layer in improving the crystal orientation of Ag(111) is greater.

In conclusion, appropriate interface layers, such as Nb and Ti nanolayers, increase the

adhesion strength of the Ag films to the SiO₂ substrates and improve the crystal orientation of Ag(111), which contributes to an improvement in the thermal stability while maintaining the low resistivity. The relevant properties of metals suited as interface layers are considered to be a large Gibbs free energy of formation for the oxide, and an appropriate atomic diameter ratio of $d_{\text{metal(fcc or hcp)}}/d_{\text{Ag}} \approx 1$, or $d_{\text{metal(bcc)}}/d_{\text{Ag}} \approx 0.866, 1.061, \text{ or } 0.919$.

Acknowledgement

This research was supported by a Grant-in-Aid (Kakenhi Grant No. 22560712) from the Japan Society for the Promotion of Science (JSPS).

References

- [1] S. Inoue, K. Okamoto, T. Nakano, J. Ohta, and H. Fujioka: Appl. Phys. Lett. **91** (2007)201920
- [2] S. D. Yambem, K. S. Liao, and S. A. Curran : Sol. Energy Mater. Sol. Cells. **95** (2011) 3060.
- [3] K. Sieradzki, K. Bailey, and T. L. Alford : Appl. Phys. Lett. **79** (2001) 3401.
- [4] H. C. Kim, T. L. Alford, and D. R. Allee: Appl. Phys. Lett. **81** (2002) 4287.
- [5] S.K. Sharma, and J. Spitz : Thin Solid Films **65** (1980) 339.
- [6] Z. Zhang, M. Kawamura, Y. Abe, and K. H. Kim: Jpn. J. Appl. Phys. **52** (2013) 078003.
- [7] Z. Wang, X. Cai, Q. Chen, and P. K. Chu: Thin Solid Films **515** (2007) 3146.
- [8] The Chemical Society of Japan: *Kagaku Binran* (Handbook of Chemistry) (Maruzen, Tokyo, 2003) 5th ed., Vol. 2. pp. 291-300 [in Japanese].

- [9] C. Kittel: *Introduction to Solid State Physics* (Wiley, New York, 2005) 8th ed., pp. 20-21.
- [10] Y. Okayama, K. Takesako, H. Kose, and K. Kawabata: The proceedings of 46th Union Conference on Vacuum (2006) p. 159 [in Japanese].
- [11] C. H. F. Peden, K. B. Kidd, and N. D. Shinn: *J. Vac. Sci. Technol. A* **9** (1991) 1518.
- [12] J. A. Venables: *Introduction to Surface and Thin Film Processes* (Cambridge University Press, Cambridge, 2000) p. 199.
- [13] Z. Nishiyama: *Sci. Rep. Tohoku Univ.* **23** (1934) 638.
- [14] G. Wassermann : *Arch. Eisenhüttenwesen* **126** (1933) 647.
- [15] G. Kurdjumov, and G. Sachs : *Z. Phys.* **64** (1930) 325.
- [16] Y. Gotoh, M. Uwaha, and I. Arai: *Appl. Surf. Sci.* **33**(1988)443.
- [17] E. Bauer, and J. Van der Merwe: *Phys. Rev. B* **33**(1986)3657.
- [18] Y. Gotoh, and H. Fukuda : *Surf. Sci.* **223**(1989) 315.

Figures

Fig. 1. SEM images of (a) Ag, (b) Ag/Pd, (c) Ag/Ni, (d) Ag/Nb, and (e) Ag/Ti films after annealing at 600 °C.

Fig. 2. Critical delamination load for as-deposited Ag, Ag/Pd, Ag/Ni, Ag/Nb, and Ag/Ti films.

Fig. 3. (Color online) (a) XRD patterns of θ -2 θ scan and (b) XRD rocking curves for as-deposited Ag, Ag/Pd, Ag/Ni, Ag/Nb, and Ag/Ti films.

Table 1. Properties of Ag, Pd, Ni, Nb, and Ti.

	Ag	Pd	Ni	Nb	Ti
Gibbs free energy of formation of oxide (kJ/mol)	-5.6 (AgO _{0.5})	-55.4 (PdO)	-211.7 (NiO)	-883.1 (NbO _{2.5})	-884.5 (TiO ₂)
Crystal structure	fcc	fcc	fcc	bcc	hcp
Close-packed plane	(111)	(111)	(111)	(110)	(0001)
Nearest-neighbor distance (nm)	0.289	0.275	0.249	0.286	0.289

Fig. 1

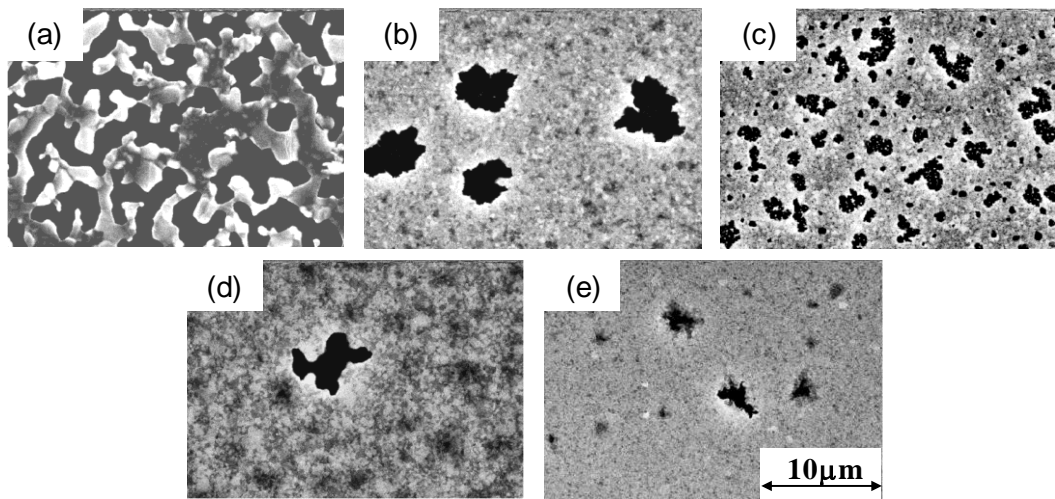


Fig. 2

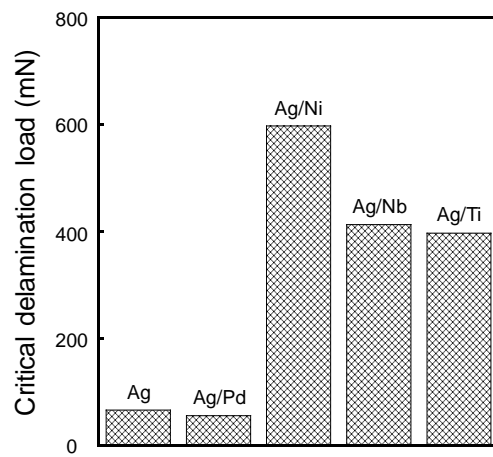
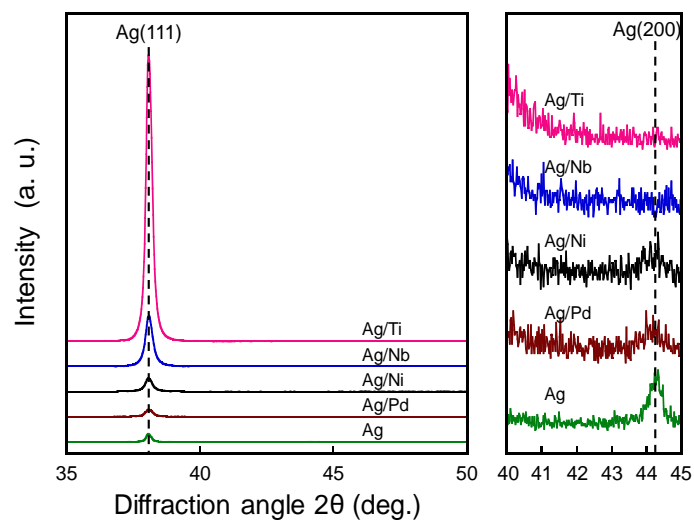
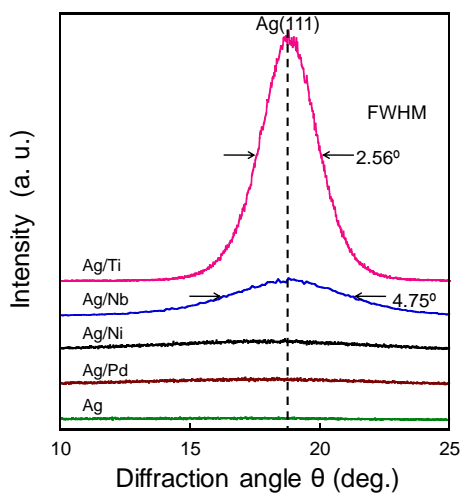


Fig. 3



(a)



(b)